Indian Journal of Chemistry
Vol. 65, April 2026, pp. 348-367
DOI: 10.56042/ijc.v65i4.26287

Greener synthesis, spectroscopical relationships, molecular docking analysis, antimicrobial, antimalarial activities of aryl *E*-imines and X-ray crystal structure of (*E*)-N-(4-nitrobenzylidene)-2-(trifluoromethyl)aniline

P Gayathri[a], P Mayavel[a,b], I Muthuvel[a,c], S Balasundari[a], P Sudha[a], J Divya[a,d], D Govindarajan[e], B Krishnakumar[f,g,h], K Ranganathan[i], V Usha[j], K Devika[k] & G Thirunarayanan*[a]

[a] Department of Chemistry, Annamalai University, Annamalinagar 608 002, Tamil Nadu, India

[b] Department of Chemistry, Government Arts College, Ariyalur 621 713, Tamil Nadu, India (Affiliated to Bharathidasan University, Tiruchirppalli 620 024, Tamil Nadu, India)

[c] Department of Chemistry, M. R. Government Arts College, Mannargudi 614 001, Tamil Nadu, India

[d] Department of Chemistry, Indra Ganesan College of Engineering College, College, Manikandam, Tiruchirappalli 620 012, Tamilnadu, India

[e] Department of Physics, Annamalai University, Annamalinagar 608 002, Tamil Nadu, India

[f] Saveetha School of Engineering, Saveetha Institute of Medical and Technical Sciences (SIMATS), Chennai 602 105, India.

[g] Department of Civil Engineering, Yeungnam University, Gyeongsan 38541, Republic of Korea.

[h] Center for Research Impacr and Outcome, Chitkara University Institute of Engineering and Technology, Chitkara University, Rajpura 140 401, Punjab, India

[i] Department of Chemistry, P. T. Lee Chengalvaraya Naickar College of Engineering & Technology, Kanchipuram 631 502, Tamil Nadu, India.

[j] Department of Chemistry, University College of Engineering Panruti, Panruti 607 106, Tamil Nadu, India

[k] Department of Chemistry, Thiru. Vi. Ka. Government Arts College, Thiruvarur 610 003, Tamil Nadu, India. (Affiliated to Bharathidasan University, Tiruchirppalli 620 024, Tamil Nadu, India)

E-mail: drgtnarayanan@gmail.com, thirunarayanan.g.10313@annamalaiuniversity.ac.in

Received 2 February 2026; accepted (revised) 7 April 2026

Three series of *E*-imines such as (*E*)-N-(substituted benzylidene)-2,3-dihydrobenzo(*b*)[1,4]-dioxin-6-amines, (*E*)-[4-(substituted benzylideneamino) phenyl] (phenyl) methanones and (*E*)-N-(substituted benzylidene)-2-(trifluoromethyl)anilines have been synthesized by sulfated fly-ash:SnO_2 catalyst assisted condensation of 2,3-dihydro(b)[1,4]dioxin-6-amine, 4-benzoylaniline, 2-trifluromethylaniline and substituted benzaldehydes under microwave irradiation conditions. This condensation gives more than 70% yield. Physicochemical constants, elemental analysis, and spectroscopical information have been applied for the characterization of synthesized *E*-imines. The X-ray single crystal structure of (*E*)-N-(4-nitrobenzylidene)-2-(trifluoromethyl) aniline **(27)** has been established. Specific spectroscopical wave numericals of the imines have been applied for QSAR linear statistical investigations. Based on the outcomes of linear QSAR computations, the influence of auxiliaries on specified spectroscopical data has been investigated. Resonance and inductive properties of the auxiliaries yield satisfactory correlations ($r > 0.900$). In molecular-docking analysis, the *E*-imines **4**, **7**, **10**, **11**, **13**, **16**, **17** and **22** show high protein-ligand interaction binding energy. The imines **5-7** and **10** show good anti-bacterial actions in contrast to *S. aureus*, *E. coli* and *P. aeruginosa* strains. In the serial dilution method, all compounds are active against their antibacterial strains. The imines **2-9**, **24** and **26** are active with MICs of 9.5-16.5 against A. *niger* microbes. Imines **4**, **5**, **14-16** and **22** exhibit good antimalarial activities against *P. falciparum* strain.

Keywords: Environmentally benign synthesis, Sulfated fly-ash:SnO_2, *E*-imines, XRD spectra, Spectral QSAR, Biological activities

Aryl or aliphatic groups bonded on both sides of -N=CH- moieties of molecules are known as imines or azomethines of Schiff bases. Concerning the lone pair electron of nitrogen and the groups in carbon atoms confirm the *E* or *Z* configuration of imines[1]. They are derived from the condensation of carbonyl compounds with anilines; then, they are called aldimines or ketamine's plentiful catalytic-substances applied for deriving *E*-imines through either conventional or greener synthetic methods. Synthetic organic chemists paid much more attention to greener synthetic methods due to the protection of the environment and high yields. From the constructive green chemical criteria, microwave irradiation with

catalyst or neat, ultrasonication, stirring in a room or low temperature, and grinding carbonyl compounds with anilines afforded high yields. The microwave-assisted synthetic method is important because it allows for the rapid and efficient heating of reactants due to its ability to produce heat directly within the reactants. It results in significantly lower reaction times compared to conventional methods. This method offers better yield and energy efficiency, making it a convenient tool in both laboratories and industries for chemical synthesis and materials science. Spectral QSAR studies delivered information about the interference of electronic properties of the auxiliaries to the characteristic spectroscopical vibrations or magnetic properties in a molecule[1]. Various metallic catalytic substances such as Pd, Ru, Au, V, Cu, Mn, and Co were utilized for the synthesis of imines. Meyer *et al*., introduced the template-directed method for imine synthesis[2]. Collados and his co-workers synthesized some *N*-tertiary butyl sulfinyl imines from tetra ethoxy titanium catalyzed greener condensation of sulfonamide and ketones[3]. The metal oxide-metal doped catalytic substances were utilized for the derivation of *E*-imines by the benzylamine self-coupler method as reported by Yu *et al*.[4] The super acid-catalyzed synthesis of some of Schiff bases through a greener synthetic method was reported by Abid and his research group[5]. Schiff bases containing Dibenzo[b, d]azepines were synthesized using [5+2] oxidative cyclization of *ortho*-substituted anilines and alkynes in the presence of Pd(II) catalyst[6]. Rizzuti *et al*., studied the influence of Fe_3O_4/CeO_2 nano reagent for *E*-imine derivation[7]. Cobalt dichloride-assisted greener synthetic strategy applied for deriving imines by dehydrogenating coupling of aryl alcohol and amines was reported by Pal *et al*.[8] Wu and his researchers investigated the imine synthesis by Zn-Alumina supported Au nanoparticle catalyzed oxidative coupling of alcohol and amines[9]. The chiral Bronsted acid catalysts employed for the synthesis of acrylic azomethine imines were published by Hashimoto *et al*.[10]

An oxide catalytic substance, hydrogen peroxide-V_2O_5, was applied for deriving imines from benzylamines[11]. A mesoporous-tungsten oxide catalytic substance was employed for greener preparations of thiazolyl imines[12]. Thirunarayanan *et al*.,[13] studied the fly-ash:H_2SO_4 assisted synthesis of some *E*-imines by the solvent-free method. Mayavel *et al*.,[14] reported the synthesis, spectral correlations, and X-ray single crystal assembly of (*E*)-N-(substituted benzylidene)-1-benzylpiperidin-4-imine derivatives. Sakthinathan and his co-workers investigated the environmentally benign synthetic strategy, antimicrobial actions, and QSAR of 2-chloro-4-methyl aniline-based Schiff bases[15]. Molecular docking analysis was applied to find the binding character of drugs to biological systems. Based on the binding energy, the medicinal activity of the drug can be explained[16]. Celik *et al*.,[17] have investigated the spectroscopical analysis, antimicrobial, and drug binding abilities of the vanillin-based imines. Recently, Dinesh kumar and his co-workers investigated the molecular docking, ADME, and biological potentials of some aryl-*E*-imines[18,19]. The azomethine and polar groups in Schiff bases exhibit numerous biological activities[18,19] and antimalarial potencies[20]. Outcomes of reviews of literature had no evidence for the environmentally benign synthetic strategies, spectroscopical QSAR, and evaluation of biological actions of 4-benzoyl aniline and 1,4-benzodioxan-6-yl imines. Hereafter, the researchers report the environmentally benign synthetic strategies, spectroscopical QSAR, and evaluation of *in vitro* bio-potencies of the above-titled compounds.

Results and Discussion

In the current research, authors took efforts for the preparation of *E*-imines by the solvent-free method using sulfated fly-ash:SnO_2 assisted reaction of aromatic amines and aldehydes under microwave irradiation conditions. This reaction yields a product percentage of more than 70. Here, the electron-donating substituents provide higher yields compared to electron-withdrawing groups. The reaction proceeds through acid-mediated nucleophilic addition, followed by the removal of water, affording imines. Initially, the carboxyl group of oxygen of the aldehyde was added a proton provided by the acidic sulfated fly-ash:SnO_2 catalyst region. This step leads to the formation of a positive charge on the carbonyl carbon. Secondly, the amino group nucleophile attacks the carbonyl carbon; then, the positive charge is created on the nitrogen atom. Stage three is loss of hydrogen, and the N atom retains the lone pair of electrons. The fourth stage is the removal of water *via* beta- elimination afforded the desired imines. The entire mechanistic steps of the condensation are illustrated in Scheme 1.

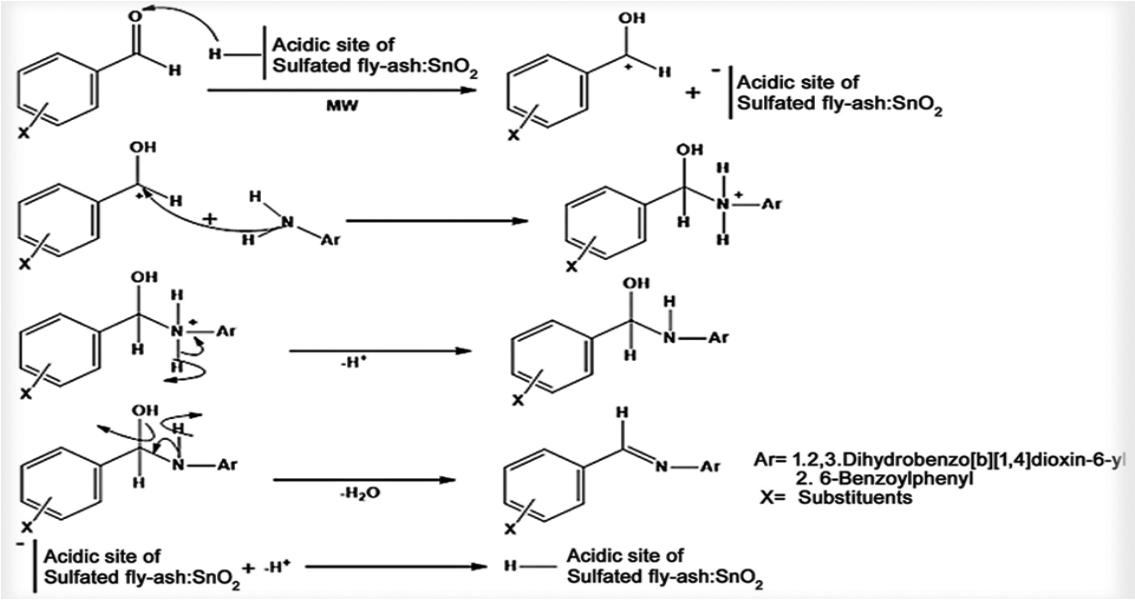

Scheme 1 — Mechanistic pathway for the synthesis of imines by sulfated fly-ash:SnO_2 catalyzed condensation of aryl amine and aldehydes under microwave irradiation conditions

In this study, the catalytic consequences of the reaction on the reaction product (Entry 1) were examined by ascending order of the quantity of catalyst as 0.05 to 0.5 g, and the quantity of product obtained in ascending order from 39 to 84% as shown in Fig. 1. Beyond 0.3 g of the catalyst, further addition did not give additional yields. From this experimentation, the ideal amount of catalyst was found to be 0.3 g.

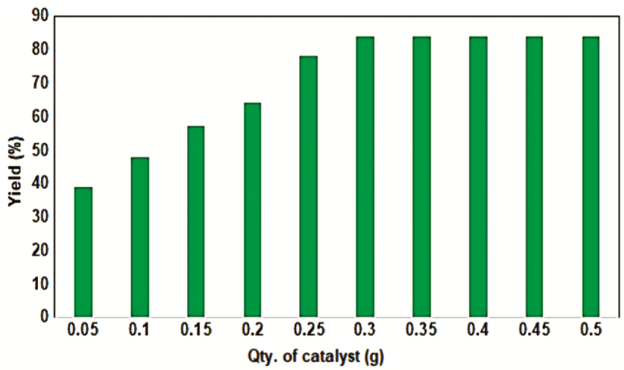

Fig. 1 — Effect of the catalyst on the yield of *E*-imine (1)

XRD structure of (*E*)-N-(4-nitrobenzylidene)-2-(trifluoromethyl)aniline, 27

All synthesized E-imines were crystallized with ethanol. The *E*-imine, (*E*)-N-(4-nitrobenzylidene)-2-(trifluoromethyl)aniline **(27)** was obtained as a transparent crystal. The X-ray diffraction experiment declared as (*E*)-N-(4-nitrobenzylidene)-2-(trifluoromethyl)aniline **(27)** possess triclinic crystal pattern with P_1 space group and the lattice data a =7.7931(4) Å, b = 11.1653(13) Å, c = 15.9278(17) Å, and α =85.838(4)°, β =79.387(4)° γ = 74.258(4)°. The lattice assembly has two imine molecules, and it has *E* geometry (CCDC No. 2377936). Lattice assembly and the geometry enhancement constraints were presented in Table 1. In the assembly structure of ORTEP, with numeration of atoms appears in Fig. 2. The investigational geometry-assembly of the packing diagram for the title imine has appeared in Fig. 3. In addition, the bond length and bond angle of the -CH=N- group is 1.262 Å N(1)-C(7) and 122.1° C(7)-N(1)-C(1) correspondingly, signifying the existence of the multi-bond moiety and these values are tabulated in Table 2.

FT-IR and NMR spectroscopical correlations

The characteristic spectroscopical frequencies of prepared *E*-imines, notably infrared C=N vibrations (ν, cm^{-1}) and the NMR chemical shifts (δ, ppm) of CH=N- moieties, were correlated against sigma numerations and Swain-Lupton's constraints[1,15,21-24] applying mono and double linear statistical computations. In these investigations, the utilized Hammett straight line equations (1) and (2) are,

$$\nu = \rho\sigma + \nu_0 \quad \ldots (1)$$

$$\delta = \rho\sigma + \delta_0 \quad \ldots (2)$$

Table 1 — The X-ray **c**rystal data and geometry enhancement constraints of (*E*)-N-(4-nitrobenzylidene)-2-(trifluoromethyl)aniline **27**

Identification code	ATF4N_090824	
Chemical formula	$C_{14}H_9F_3N_2O_2$	
Formula weight	294.23 g/mol	
Temperature	300(2) K	
Wavelength	0.71073 Å	
Crystal size	0.040×0.192×0.216 mm	
Crystal habit	colorless block	
Crystal system	triclinic	
Space group	P -1	
Unit cell dimensions	a = 7.7931(9) Å	α = 85.838(4)°
	b = 11.1653(13)Å	β = 79.387(4)°
	c = 15.9278(17) Å	γ = 74.258(4)°
Volume	1310.7(3) $Å^3$	
Z	4	
Density (calculated)	1.491 g/cm^3	
Absorption coefficient	0.130 mm^{-1}	
F(000)	600	
Theta range for data collection	1.90 to 28.43°	
Index ranges	-10<=h<=10, -14<=k<=14, -21<=l<=21	
Reflections collected	54029	
Independent reflections	6541 [R(int) = 0.0630]	
Coverage of independent reflections	99.1%	
Absorption correction	Numerous scan	
Max. and min. transmission	0.9950 and 0.9730	
Structure solution technique	direct methods	
Structure solution program	XT, VERSION 2018/2	
Refinement method	Full-matrix least-squares on F2	
Refinement program	SHELXL-2019/1 (Sheldrick, 2019)	
Function minimized	Σ w(Fo2 - Fc2)2	
Data / restraints / parameters	6541 / 0 / 380	
Goodness-of-fit on F2	1.020	
Final R indices	3416 data; I>2σ(I)	R1 = 0.0526, wR2 = 0.1370
	all data	R1 = 0.1180, wR2 = 0.1850
Weighting scheme	$w=1/[\sigma^2(F_o^2)+(0.0772P)^2+0.3727P]$ where $P=(F_o^2+2F_c^2)/3$	
Extinction coefficient	0.0250(30)	
Largest diff. peak and hole	0.205 and -0.193 $eÅ^{-3}$	
R.M.S. deviation from mean	0.046 $eÅ^{-3}$	
(CCDC No. 2377936)		

Where ν_0 and δ_0 are the spectral frequencies of the parent series of the synthesized imines.

The statistical results of the above-said spectral frequencies against sigma numerical constants and Swain-Lupton's constraints[24] are presented in Table S1 (Supplementary Information for full details statistical analysis result).

The stretching vibrations ($\nu_{C=N}$, cm^{-1}) of (*E*)-N-substituted benzylidene-2,3-dihydrobenzo(*b*)[1,4]-dioxin-6-amines (**1-11**) produced acceptable correlation coefficients against sigma substituent numerical constants σ_R (r = 0.906) and R (r = 0.906). The rest of the sigma substituent numerical constants σ, σ^+, σ_I, and F failed in correlations. Failure in regression occurred by non-ideal polarity, inductiveness, and space effect properties of substituent groups, accompanied with resonative-conjugativeness geometry as illustrated in Fig. 4.

A ^1H chemical shifts (δ, ppm) -CH=N- of (*E*)-N-substituted benzylidene-2,3-dihydrobenzo(*b*)[1,4]-dioxin-6-amines (**1-11**) produced acceptable correlations against σ_R (r = 0.900) and R (r = 0.904) parameters, excluding 4-F and 2-CH_3 substituents. The rest of the substituent numerical factors

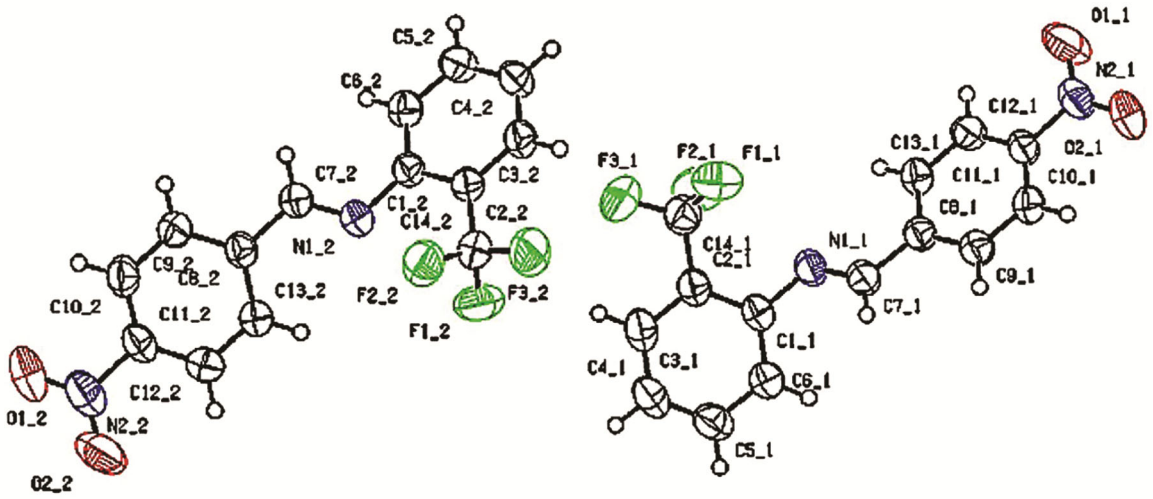

Fig. 2 — ORTEP structure of (*E*)-N-(4-nitrobenzylidene)-2-(trifluoromethyl)aniline **(27).**

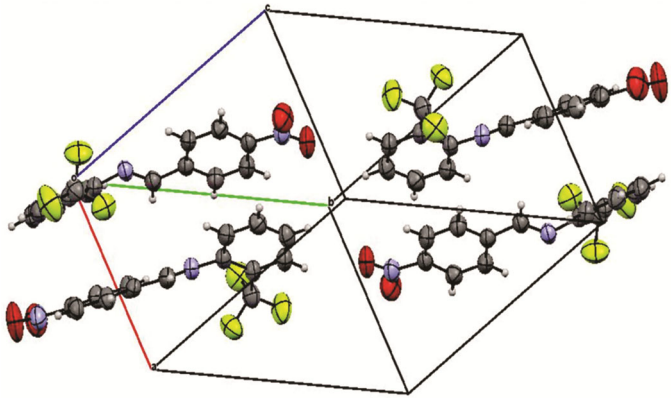

Fig. 3 — Packing diagram of (*E*)-N-(4-nitrobenzylidene)-2-(trifluoromethyl)aniline **(27).**

Table 2 — Bond length [Å] and bond angles [°] of (*E*)-N-(4-nitrobenzylidene)-2-(trifluoromethyl)aniline **27**

Bond lengths (Å)			
Atom	XRD	Atom	DFT
F1_1-C14_1	1.331(3)	F2_1-C14_1	1.327(3)
F3_1-C14_1	1.326(3)	O1_1-N2_1	1.210(3)
O2_1-N2_1	1.219(3)	N1_1-C7_1	1.267(3)
N1_1-C1_1	1.416(3)	N2_1-C11_1	1.468(3)
C1_1-C6_1	1.386(3)	C1_1-C2_1	1.403(3)
C2_1-C3_1	1.390(3)	C2_1-C14_1	1.491(3)
C3_1-C4_1	1.374(4)	C3_1-H3_1	0.930000
C4_1-C5_1	1.368(3)	C4_1-H4_1	0.930000
C5_1-C6_1	1.383(3)	C5_1-H5_1	0.930000
C6_1-H6_1	0.930000	C7_1-C8_1	1.469(3)
C7_1-H7_1	0.930000	C8_1-C13_1	1.384(3)
C8_1-C9_1	1.387(3)	C9_1-C10_1	1.379(3)
C9_1-H9_1	0.930000	C10_1-C11_1	1.369(3)
C10_1-H10_1	0.930000	C11_1-C12_1	1.376(3)
C12_1-C13_1	1.377(3)	C12_1-H12_1	0.930000
C13_1-H13_1	0.930000	F1_2-C14_2	1.329(3)

(*Contd.*)

Table 2 — Bond length [Å] and bond angles [°] of (*E*)-N-(4-nitrobenzylidene)-2-(trifluoromethyl)aniline **27** (*Contd*.)

Bond lengths (Å)			
Atom	XRD	Atom	DFT
F2_2-C14_2	1.338(3)	F3_2-C14_2	1.333(3)
O1_2-N2_2	1.205(3)	O2_2-N2_2	1.216(3)
N1_2-C7_2	1.262(3)	N1_2-C1_2	1.414(3)
N2_2-C11_2	1.472(3)	C1_2-C6_2	1.388(3)
C1_2-C2_2	1.404(3)	C2_2-C3_2	1.386(3)
C2_2-C14_2	1.490(3)	C3_2-C4_2	1.375(3)
C3_2-H3_2	0.930000	C4_2-C5_2	1.375(3)
C4_2-H4_2	0.930000	C5_2-C6_2	1.381(3)
C5_2-H5_2	0.930000	C6_2-H6_2	0.930000
C7_2-C8_2	1.468(3)	C7_2-H7_2	0.930000
C8_2-C9_2	1.382(3)	C8_2-C13_2	1.394(3)
C9_2-C10_2	1.379(3)	C9_2-H9_2	0.930000
C10_2-C11_2	1.370(3)	C10_2-H10_2	0.930000
C11_2-C12_2	1.374(3)	C12_2-C13_2	1.371(3)
C12_2-H12_2	0.930000	C13_2-H13_2	0.930000
Bond angles (°)			
Atom	XRD	Atom	DFT
C7_1-N1_1-C1_1	118.98(19)	O1_1-N2_1-O2_1	123.4(2)
O1_1-N2_1-C11_1	118.5(2)	O2_1-N2_1-C11_1	118.1(2)
C6_1-C1_1-C2_1	118.79(19)	C6_1-C1_1-N1_1	122.77(19)
C2_1-C1_1-N1_1	118.37(19)	C3_1-C2_1-C1_1	119.5(2)
C3_1-C2_1-C14_1	120.2(2)	C1_1-C2_1-C14_1	120.27(19)
C4_1-C3_1-C2_1	120.6(2)	C4_1-C3_1-H3_1	119.700000
C2_1-C3_1-H3_1	119.700000	C5_1-C4_1-C3_1	120.1(2)
C5_1-C4_1-H4_1	120.000000	C3_1-C4_1-H4_1	120.000000
C4_1-C5_1-C6_1	120.3(2)	C4_1-C5_1-H5_1	119.800000
C6_1-C5_1-H5_1	119.800000	C5_1-C6_1-C1_1	120.7(2)
C5_1-C6_1-H6_1	119.700000	C1_1-C6_1-H6_1	119.700000
N1_1-C7_1-C8_1	122.1(2)	N1_1-C7_1-H7_1	118.900000
C8_1-C7_1-H7_1	118.900000	C13_1-C8_1-C9_1	119.53(19)
C13_1-C8_1-C7_1	121.17(19)	C9_1-C8_1-C7_1	119.3(2)
C10_1-C9_1-C8_1	120.4(2)	C10_1-C9_1-H9_1	119.800000
C8_1-C9_1-H9_1	119.800000	C11_1-C10_1-C9_1	118.6(2)
C11_1-C10_1-H10_1	120.700000	C9_1-C10_1-H10_1	120.700000
C10_1-C11_1-C12_1	122.37(19)	C10_1-C11_1-N2_1	118.8(2)
C12_1-C11_1-N2_1	118.7(2)	C11_1-C12_1-C13_1	118.6(2)
C11_1-C12_1-H12_1	120.700000	C13_1-C12_1-H12_1	120.700000
C12_1-C13_1-C8_1	120.4(2)	C12_1-C13_1-H13_1	119.800000
C8_1-C13_1-H13_1	119.800000	F3_1-C14_1-F2_1	106.0(2)
F3_1-C14_1-F1_1	106.2(2)	F2_1-C14_1-F1_1	104.9(2)
F3_1-C14_1-C2_1	112.5(2)	F2_1-C14_1-C2_1	113.0(2)
F1_1-C14_1-C2_1	113.6(2)	C7_2-N1_2-C1_2	119.87(18)
O1_2-N2_2-O2_2	123.5(2)	O1_2-N2_2-C11_2	117.9(3)
O2_2-N2_2-C11_2	118.5(2)	C6_2-C1_2-C2_2	118.64(19)
C6_2-C1_2-N1_2	122.46(19)	C2_2-C1_2-N1_2	118.75(19)
C3_2-C2_2-C1_2	119.7(2)	C3_2-C2_2-C14_2	119.9(2)
C1_2-C2_2-C14_2	120.42(19)	C4_2-C3_2-C2_2	120.7(2)
C4_2-C3_2-H3_2	119.600000	C2_2-C3_2-H3_2	119.600000
C3_2-C4_2-C5_2	119.8(2)	C3_2-C4_2-H4_2	120.100000
C5_2-C4_2-H4_2	120.100000	C4_2-C5_2-C6_2	120.3(2)
C4_2-C5_2-H5_2	119.900000	C6_2-C5_2-H5_2	119.900000
C5_2-C6_2-C1_2	120.8(2)	C5_2-C6_2-H6_2	119.600000

(*Contd*.)

Table 2 — Bond length [Å] and bond angles [°] of (*E*)-N-(4-nitrobenzylidene)-2-(trifluoromethyl)aniline **27** (*Contd*.)

Bond lengths (Å)			
Atom	XRD	Atom	DFT
C1_2-C6_2-H6_2	119.600000	N1_2-C7_2-C8_2	121.1(2)
N1_2-C7_2-H7_2	119.400000	C8_2-C7_2-H7_2	119.400000
C9_2-C8_2-C13_2	119.31(19)	C9_2-C8_2-C7_2	120.64(19)
C13_2-C8_2-C7_2	120.05(18)	C10_2-C9_2-C8_2	120.7(2)
C10_2-C9_2-H9_2	119.700000	C8_2-C9_2-H9_2	119.700000
C11_2-C10_2-C9_2	118.5(2)	C11_2-C10_2-H10_2	120.700000
C9_2-C10_2-H10_2	120.700000	C10_2-C11_2-C12_2	122.3(2)
C10_2-C11_2-N2_2	119.6(2)	C12_2-C11_2-N2_2	118.1(2)
C13_2-C12_2-C11_2	118.8(2)	C13_2-C12_2-H12_2	120.600000
C11_2-C12_2-H12_2	120.600000	C12_2-C13_2-C8_2	120.4(2)
C12_2-C13_2-H13_2	119.800000	C8_2-C13_2-H13_2	119.800000
F1_2-C14_2-F3_2	105.64(19)	F1_2-C14_2-F2_2	106.0(2)
F3_2-C14_2-F2_2	105.5(2)	F1_2-C14_2-C2_2	113.1(2)
F3_2-C14_2-C2_2	112.2(2)	F2_2-C14_2-C2_2	113.84(19)
CCDC No. 2377936			

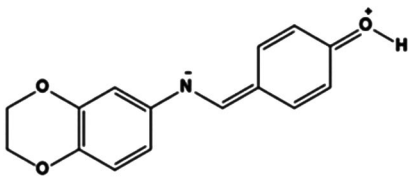

Fig. 4 — The resonance-conjugative structure

(σ, σ^+, σ_I) and F gave poor regression coefficients. The entire correlations produced negative ρ quantities excluding σ_R and R, and it denotes that the opposite displacement effect operates to imine systems. The poor and opposite effect observed in imine compounds is due to the reason stated earlier and the accomplishment of Fig. 4.

Azomethine -CH=N- carbon chemical shifts (δ, ppm) of (*E*)-N-substituted benzylidene-2,3-dihydrobenzo(*b*)[1,4]-dioxin-6-amines **(1-11)** produced normal regression coefficients against sigma substituent numerical constants (σ, σ^+, σ_I, σ_R), F and R excepting H, 4-F, 3-OCH_3 and 2-CH_3 substituents. Inclusion of these auxiliaries in the regression diminished the regression coefficients significantly. The entire regression produces opposite ρ quantities, and it demonstrates the opposite displacement characters operated in the imine compounds and is associated with the resonated-conjugativeness geometry of Fig. 4.

In mono-regressions, many statistical outcomes have poor correlation coefficients for the imines (**1-11**). While seeking the outcome of statistical double-regressions produced normal regression coefficients against sigma numerical constants, F and R Swain-Lupton's parameters[24]. The obtained double regression equations (3-8) for the imines (**1-11**) are,

$$\nu_{C=N}\ (cm^{-1}) = 1581.46\ (\pm 2.134) + 1.646\ (\pm 0.420)\sigma_I - 11.214\ (\pm 4.492)\sigma_R$$
$$(R = 0.960,\ n = 11,\ P > 95\%) \quad \ldots (3)$$

$$\nu_{C=N}\ (cm^{-1}) = 1581.21\ (\pm 1.949) + 1.911\ (\pm 0.384)\ F - 8.493\ (\pm 3.291)\ R$$
$$(R = 0.967,\ n = 11,\ P > 95\%) \quad \ldots (4)$$

$$\delta_{CH=N}\ (ppm) = 8.577\ (\pm 0.072) - 0.232\ (\pm 0.122)\sigma_I + 0.290\ (\pm 0.152)\sigma_R$$
$$(R = 0.962,\ n = 11,\ P > 95\%) \quad \ldots (5)$$

$$\delta_{CH=N}\ (ppm) = 8.550\ (\pm 0.070) - 0.164\ (\pm 0.082)\ F + 0.188\ (\pm 0.092)\ R$$
$$(R = 0.956,\ n = 11,\ P > 95\%) \quad \ldots (6)$$

$$\delta_{C=N}\ (ppm) = 158.16\ (\pm 0.345) - 3.553\ (\pm 0.680)\sigma_I - 2.153\ (\pm 0.726)\sigma_R$$
$$(R = 0.992,\ n = 11,\ P > 95\%) \quad \ldots (7)$$

$$\delta_{C=N}\ (ppm) = 158.02\ (\pm 0.344) - 3.395\ (\pm 0.678)\ F - 2.157\ (\pm 0.581)\ R$$
$$(R = 0.991,\ n = 11,\ P > 95\%) \quad \ldots (8)$$

Molecular docking analysis

Outcome of the docked experiments of synthesized (*E*)-N-(substituted benzylidene)-2,3-dihydrobenzo(*b*)[1,4]-dioxin-6-amines **(1-11)**, (*E*)-[4-(substituted benzylideneamino) phenyl](phenyl) methanones (**12-23**) and (*E*)-N-(substituted benzylidene)-2-(trifluoromethyl)anilines **(24-27)**

HER2 protein inhibitor 7PCD and they produced -5.19 to -8.38 kcal/mol of binding energies. Compound **4** shows binding energy values of -6.14 kcal/mol and also shows one hydrogen bond interaction through residue of amino acid TYR A:772 (Tyrosine), three hydrophobic bond interactions such as ALA A:775, LEU A:785, and MET A:774 (Alanine, Leucine, and Methionine). Compound **7** shows binding energy values -6.14 kcal/mol implies one hydrophobic bond interaction through residue of amino acid PRO A:983 (Proline), dual electrostatic bond interactions to ARG A:981 and ASP A:982 (Arginine and Aspartic acid), and one hydrogen bond interaction to GLN A:820 (Glutamine). The compound **10** shows binding energy values -6.25 kcal/mol and also shows two hydrophobic bond interactions to amino acid residues VAL A: 777 and PRO A:780 (Valine and Proline). There are thrice electrostatic bond interactions to ARG A:784 and LYS A:854, LYS A:860 (Arginine and Lysine) and one hydrogen bond interaction to HIS A:858 (Histidine). The compound **11** shows -6.27 kcal/mol binding energy and it demonstrates one hydrophobic bond interaction to the residue of amino acid VAL A:777 (Valine). Thrice electrostatic bond interactions to ARG A:784, LYS A:854, LYS A:860 (Arginine and Lysine) and two hydrogen bond interaction to HIS A:858, GLN A:799 (Histidine and Glutamine).The imine **13** shows binding energy values -8.38 kcal/mol and also shows one electrostatic bond interaction with amino acid residues such as ASP A:924 (Aspartic acid), five hydrophobic bond interactions such as ALA A:920, ILE A:926, LEU A:934, TRP A:913, PRO A:942 (Alanine, Isoleucine, Leucine, Tryptophan and Proline). Compound **16** shows the binding energy value -8.27 kcal/mol, it demonstrates one hydrophobic bond interaction to the residue of amino acids ALA A:867, LEU A:866, PHE A:899, and PRO A:983 (Alanine, Leucine, Phenylalanine, and Proline). There are three electrostatic bond interactions that occur to ARG A:844, ARG A:897, ARG A:898 (Arginine). Compound **17** shows the binding energy value of -8.21 kcal/mol it demonstrates three electrostatic bond forces to the residue of amino acids ARG A:844, ARG A:897, and ASP A:845 (Arginine and Aspartic acid) and three hydrophobic bond attractive forces occurred to ALA A:730, ALA A:867, GLY A:865, (Alanine, Glycine). The compound **22** shows the binding energy of -8.17 kcal/mol, it demonstrates one hydrophobic bond forces occurred to residues of amino acid PRO A:856 (Proline), two electrostatic bond forces existed to the residues of amino acids GLU A:812 and LYS A:736 (Glutamic acid and Lysine) and two hydrogen bond forces of attractions occurred to ASN A:813 and TYR A:803 (Asparagine and Tyrosine) residues of amino acids. The two- and three-dimensional docking poses of compounds **4**, **7**, **10**, **11**, **13**, **16**, **17**, and **22** are shown in Table 3.

Antimicrobial activity

Anti-bacterial activity

Assessed antibacterial potencies through measurement of mm of zone of inhibition of (*E*)-N-substituted benzylidene-2,3-dihydrobenzo(*b*)[1,4]-dioxin-6-amines **1-11** and (*E*)-N-(substituted benzylidene)-2-(trifluoromethyl)anilines **24-27** are presented in Table 4. The disc contained a zone of inhibitions[15,16,18,19,21] of imines **1-11**, which are shown in Fig. 5, and the statistical clustered column chart **1-11** and **24-27** of the imines are depicted in Fig. 6.

The (*E*)-N-substituted benzylidene-2,3-dihydrobenzo(*b*)[1,4]-dioxin-6-amines **2-11** and N-(substituted benzylidene)-2-(trifluoromethyl)anilines **24-27** produced reasonable anti-bacterial actions against *B. subtilis*. Here, the electronegativity of F, inductive effects of bromo, methoxy, nitro, inductive and mesomeric effects of methyl substituents, partially encouraged the antibacterial activity against their strains. The parent compound **1** with the substituent as H shows the least anti-bacterial actions in contrast to *B. subtilis* strain due to the +I consequences of aryl rings, unable to predict the bacterial activity against the microbe. (*E*)-N-(4-chlorobenzylidene)-2,3-dihydrobenzo(*b*)[1,4]-dioxin-6-amine **5** exhibited good. The remaining compounds **1-3**, **5-11** and **24-26** showed moderate antibacterial activity against the *S. aureus* strain. (*E*)-N-(4-nitrobenzylidene)-2-(trifluoromethyl) aniline **27** shows the least antibacterial activity. Here, the +I character of the chlorine substituent enhances the antibacterial activity, remaining substituents partially predict the activity, and the compound **27** possesses a 4-NO_2 group and which lowers the antibacterial activity by its inductive effect and electron-withdrawing character. Schiff base **10** with –I effect and electron-withdrawing nature of 3-NO_2 group produced good anti-bacterial potencies, compounds **3-7**, **9**, **11**, **24-27** with the substituents 4-Br, 3-Cl, 4-Cl, 4-F, 4-OH, 2-CH_3, 4-NO_2 produced modest actions in contradiction to *S. pyogenes*. The reason for modest

Table 3 — The 2D and 3D structures of *E*-imines, along with binding energy(ΔG) kcal/mol

Entry	2D docked geometry	3D docked geometry	Binding energy
	(*E*)-N-(Substituted benzylidene)-2,3-dihydrobenzo(*b*)[1,4]-dioxin-6-amines		
4	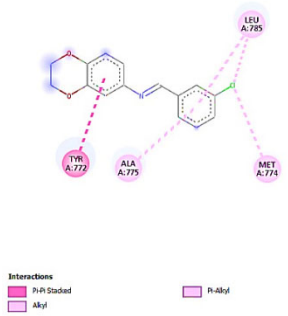	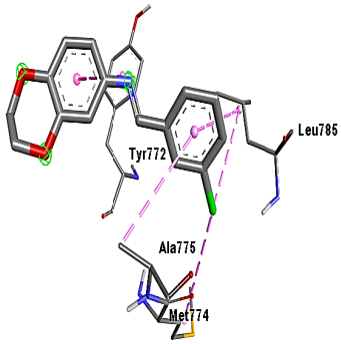	-6.14
7	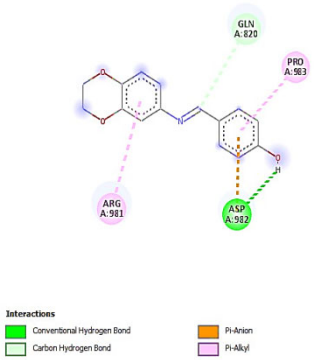	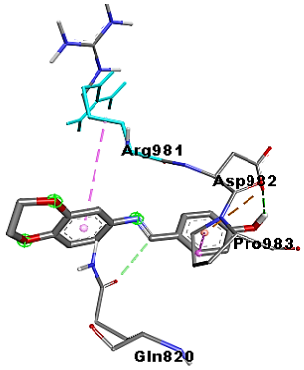	-6.14
10	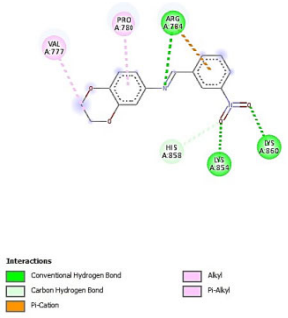	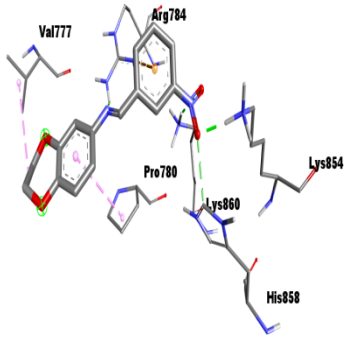	-6.25
11	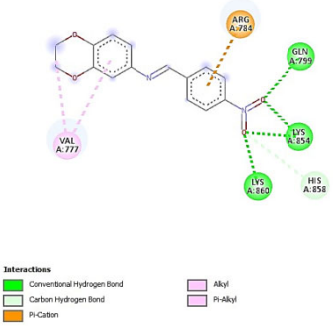	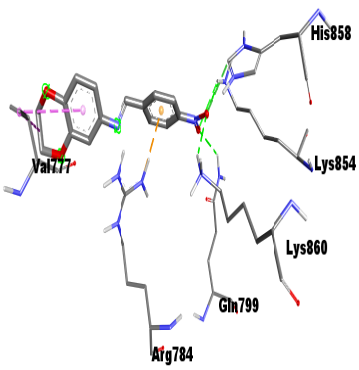	-6.27

(*Contd.*)

(*E*)-[4-(Substituted benzylideneamino)phenyl](phenyl)methanones

Table 3 — The 2D and 3D structures of E-imines, along with binding energy(ΔG) kcal/mol (*Contd.*)

Entry	2D docked geometry	3D docked geometry	Binding energy
	(*E*)-N-(Substituted benzylidene)-2,3-dihydrobenzo(*b*)[1,4]-dioxin-6-amines		
13	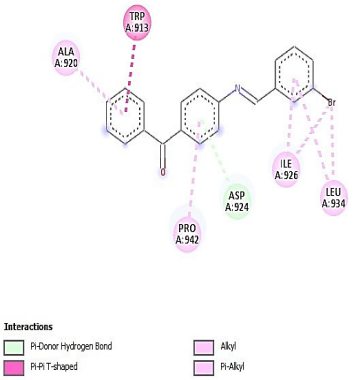	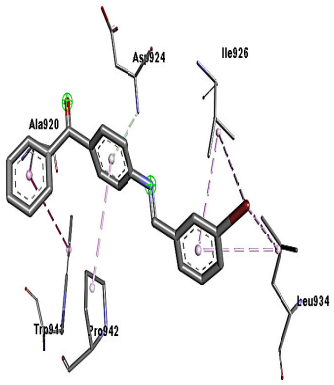	-8.38
16	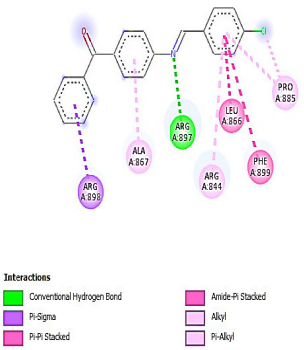	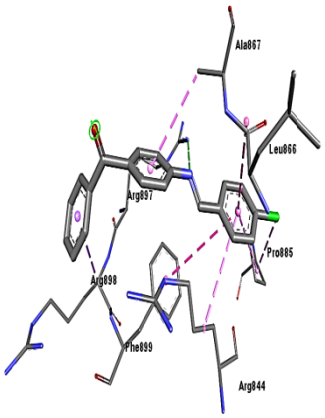	-8.27
17	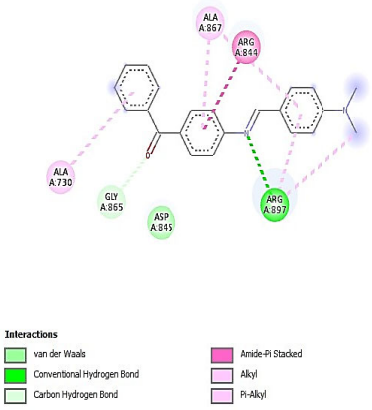	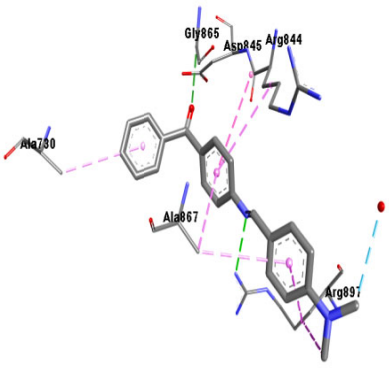	-8.21

(*Contd.*)

Table 3 — The 2D and 3D structures of *E*-imines, along with binding energy(ΔG) kcal/mol (*Contd*.)

Entry	2D docked geometry	3D docked geometry	Binding energy
	(*E*)-N-(Substituted benzylidene)-2,3-dihydrobenzo(*b*)[1,4]-dioxin-6-amines		
22	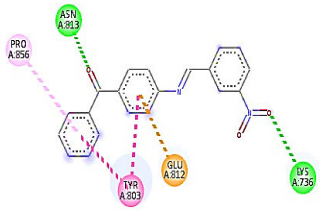	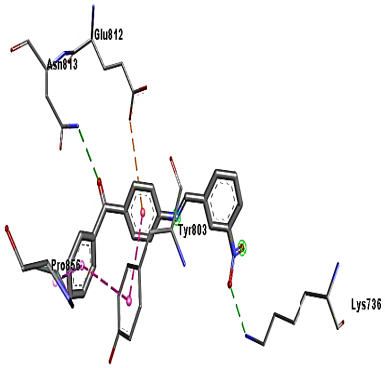	-8.17

Table 4 — Antibacterial potencies of (*E*)-N-(substituted benzylidene)-2,3-dihydrobenzo(*b*)[1,4]- dioxin-6-amines (**1-11**) and (*E*)-N-(substituted benzylidene)-2-(trifluoromethyl)anilines (**24-27**).

Entry	X	Measured mm of zone of inhibition				
		Gram-positive			Gram-negative	
		B. subtilis	*S. aureus*	*S. pyogenes*	*E. coli*	*P. aeruginosa*
		(*E*)-N-substituted benzylidene-2,3-dihydrobenzo(*b*)[1,4]-dioxin-6-amines				
1	H	7	15	9	15	13
2	3-Br	17	16	–	18	13
3	4-Br	17	12	12	19	14
4	3-Cl	14	17	13	18	14
5	4-Cl	13	29	12	14	17
6	4-F	15	13	15	22	–
7	4-OH	15	15	12	27	12
8	3-OCH_3	15	16	–	12	12
9	2-CH_3	15	14	15	17	13
10	3-NO_2	12	15	21	17	10
11	4-NO_2	15	13	11	19	12
		(*E*)-N-(substituted benzylidene)-2-(trifluoromethyl)anilines				
24	2-Br	15	16	14	15	16
25	4-Cl	13	15	11	9	11
26	3-NO_2	11	13	11	11	13
27	4-NO_2	12	10	10	12	9
Standard: Ciprofloxacin		32	33	28	30	33

actions was narrated previously. The parent compound **1** shows the least antibacterial activity, and this is associated with the +I effect of the aryl ring.

Imines **(2)** and **(8)** were inactive in showing antibacterial activity against the *S. pyogenes* strain. This is due to the –I effect of 3-Br and +I effect of 3-OCH_3 groups inhibit the antibacterial activity. The imines (**6** and **7**) show respectable anti-bacterial actions in contrast to the *E. coli* strain. The rest of the imines show moderate activity. The Schiff base **(25)** shows the least antibacterial activity. Here, the electronegativity of F and the +I character of the hydroxy auxiliaries, which enhances the actions. The positive inductive effect of the chlorine atom in imine **(25)** reduces the antibacterial activity. The synthesized imines **(1-5**, **7-11**, **24-26)** show moderate antibacterial activity against the *P. aeruginosa microbe.* Imine (**27)** shows the least activity against microorganisms due to the –I effect, and the inadequate electronic nature of the nitro auxiliary

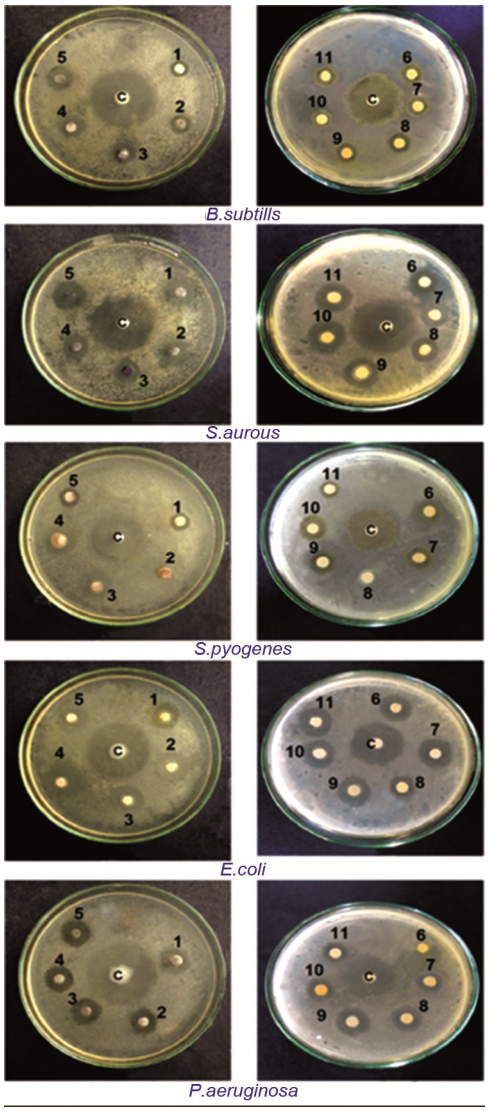

Fig. 5 — Antibacterial activities (Petri-dishes) of (*E*)-N-(substituted benzylidene)-2,3-dihydrobenzo(*b*)[1,4]-dioxin-6-amines **1-11**

reduces the activity. Fluorinated imine (6) is inactive for showing antibacterial activity against the *P. aeruginosa* strain, and this is due to the electronegativity of the F atom inhibiting the activity.

Almost all prepared *E*-mines (**1-11**) and (**24-27**) show 50% antibacterial activity against their microbes. Therefore, the authors moved to evaluate the antibacterial activity of the above imines using the determination of MIC using a two-fold serial dilution method. The assessed minimum inhibitory concentration (MIC) of the *E*-mines (**1-11**) and (**24-27**) were tabulated in Table S2(Supplementary Information).

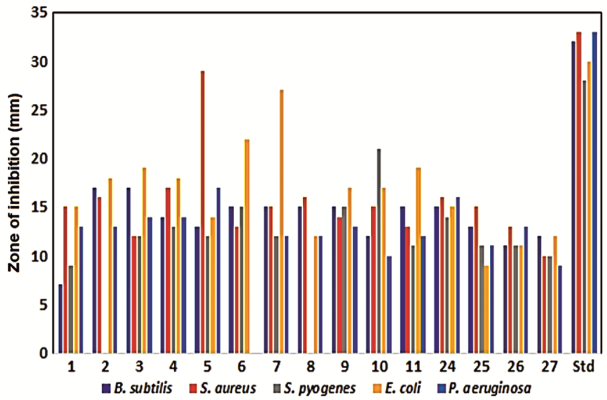

Fig. 6 — Antibacterial activities-clustered column chart of (*E*)-N-(substituted benzylidene)-2,3 dihydrobenzo(*b*)[1,4]-dioxin-6-amines **1-11** and (*E*)-N-(substituted benzylidene)-2-(trifluoromethyl)anilines **24-27**

The antibacterial activities using MIC of *E*-imines **2-6**, **8**, **9**, **24**, and **25** were active with the MIC range of 6-9 against the *B. subtilis strain* compared with the standard 5.5. The same compounds are active with the MIC range of 5.5-9 against the *S. aureus* microorganism compared with 6.15. The electronegativity of fluorene and the inductive character of bromo, methoxy, methyl, and nitro groups enhanced the bacterial actions. The halo substituted, methoxy and methyl substituted above imines active with the MICs range of 8.5-11 against *S. pyogenes* strains possess a 7 standard MIC. Here, the –I and +I effect of -OCH_3 and -CH_3 groups boosted the antibacterial actions. Similarly, above compounds show reasonable actions against *E. Coli* and *P. aeruginosa* microbes with the MIC range of 9-12 compared with their standard MIC of 7.25-6.

Antifungal potencies

Assessed fungal potencies through the measurement of mm of the zone of dedevelopment of fungal organisms[15,16,18,19,21]. Of all of (*E*)-N-substituted benzylidene-2,3-dihydrobenzo(*b*)[1,4]-dioxin-6-amines **(1-11)** and (*E*)-N-(substituted benzylidene)-2-(trifluoromethyl)anilines **(24-27)** are tabulated in Table 5. The assessed anti-fungal actions in petri dishes of imines **1-11** are illustrated in Fig. 7, and Fig. 8 illustrates the clustered column charts of imines **1-11** and **24-27**.

The (*E*)-N-(substituted benzylidene)-2,3-dihydrobenzo(*b*)[1,4]-dioxin-6-amines **1-4**, **6-11** and (*E*)-N-(substituted benzylidene)-2-(trifluoromethyl) anilines **26** and **27** shows modest anti-fungal actions in contradiction with *A. niger* strain. It happened by

Table 5 — Antifungal activities of (*E*)-N-(substituted benzylidene)-2,3-dihydrobenzo(*b*) [1,4]-dioxin-6-amines **1-11** and (*E*)-N-(substituted benzylidene)-2-(trifluoromethyl)anilines **24-27**.

Entry	X	Assessed the mm of zone of inhibition		
		A. niger	*F. oxysporum*	*P. chrysogenum*
(*E*)-N-substituted benzylidene-2,3-dihydrobenzo(*b*)[1,4]-dioxin-6-amines				
1	H	16	11	9
2	3-Br	12	14	–
3	4-Br	12	14	7
4	3-Cl	12	15	–
5	4-Cl	–	8	–
6	4-F	10	11	10
7	4-OH	9	12	11
8	3-OCH_3	12	11	11
9	2-CH_3	12	15	11
10	3-NO_2	13	15	9
11	4-NO_2	14	14	14
(*E*)-N-(substituted benzylidene)-2-(trifluoromethyl)anilines				
24	2-Br	8	9	10
25	4-Cl	4	10	6
26	3-NO_2	11	14	12
27	4-NO_2	13	15	13
Standard: Clotrimazole		32	32	32

the fluorine atom's electronegativity, inductive effects of bromo, methoxy, nitro, inductive and mesomeric effects of methyl substituents partially encouraged the antibacterial fungal activity against their strain. The imines **6, 24** and **25** show least activity and imine **5** is inactivate referred to *A. niger* strain. Here, the +I effect of 4-OH, Cl, and Br substituents diminished antifungal actions. Aryl (*E*)-imines **1-4**, **6-11**, and **25-27** showed moderate antifungal activity against the *F. oxysporum* fungal strain. Imines **(5)** and **(24)** show the least activity due to the +I effect of chloro and bromo substituents, reducing the antifungal activity. The synthesized imines **1**, **3**, **6-9**, **11**, **24**, **26**, and **27** possess modest antifungal actions in contradiction with the *P. chrysogenum* organism. Schiff bases **1**, **10**, and **25** show the least antifungal activity due to the +I effect of the aryl ring, bromo, chloro, and the positive character of nitro auxiliary reduces antifungal actions. *E*-imines **2**, **4**, and **5** inactive for showing antifungal activity against *P. chrysogenum* fungal microbe by the +I character of bromine and chlorine auxiliaries.

From the two-fold serial dilution method, with the MIC values in Table S2 (Supplementary Information), the antifungal activities of halogens, hydroxy, methoxy, and methyl-substituted *E*- imines **2-9**, **24** and **26** were active with MICs of 9.5-16.5 against A. *niger* microbes compared with the standard MIC of

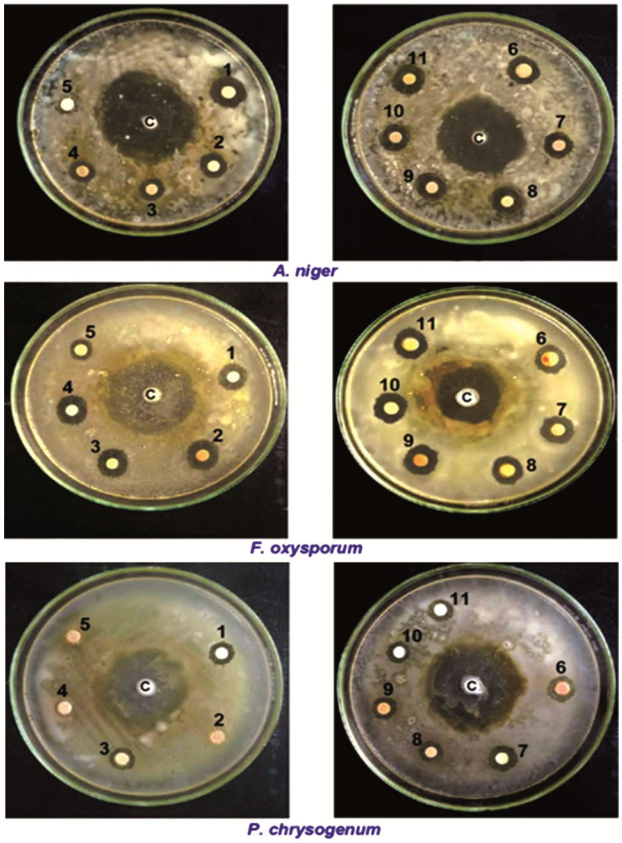

Fig. 7 — Antifungal activities (Petri-dishes) of (*E*)-N-substituted benzylidene-2,3-dihydrobenzo(*b*)[1,4]-dioxin-6-amines **1-11**

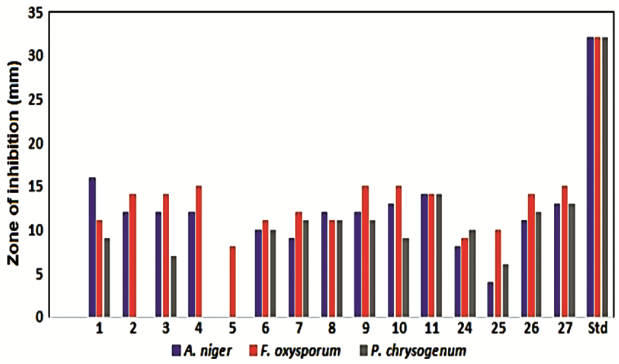

Fig. 8 — Antifungal activities-clustered column chart of (*E*)-N-(substituted benzylidene)-2,3-dihydrobenzo(*b*)[1,4]-dioxin-6-amines **1-11** and (*E*)-N-(substituted benzylidene)-2-(trifluoromethyl)anilines **24-27**

10.5. Similarly, the same imines were active with the MIC value range of 8.5-20 against *F. oxysporum* and *P. chrysogenum* strains with standard MICs of 14.25 and 13.25. The remaining imines were least active against their strains compared with lower potency. The reason for active fungal action was stated earlier. The potency was calculated by the following formula.

Table 6 — Measured antimalarial activities of *E*-imines

Entry	Ar	X	Binding energy
1	2,3-Dihydrobenzo[b][1,4]dioxin-6-amine	H	22.34±0.17
2	2,3-Dihydrobenzo[b][1,4]dioxin-6-amine	3-Br	32.33±0.27
3	2,3-Dihydrobenzo[b][1,4]dioxin-6-amine	4-Br	33.03±0.11
4	2,3-Dihydrobenzo[b][1,4]dioxin-6-amine	3-Cl	36.12±0.32
5	2,3-Dihydrobenzo[b][1,4]dioxin-6-amine	4-Cl	36.02±0.43
6	2,3-Dihydrobenzo[b][1,4]dioxin-6-amine	4-F	34.12±0.34
7	2,3-Dihydrobenzo[b][1,4]dioxin-6-amine	4-OH	26.12±0.45
8	2,3-Dihydrobenzo[b][1,4]dioxin-6-amine	3-OCH_3	25.38±0.32
9	2,3-Dihydrobenzo[b][1,4]dioxin-6-amine	2-CH_3	25.03±0.22
10	2,3-Dihydrobenzo[b][1,4]dioxin-6-amine	3-NO_2	31.62±0.16
11	2,3-Dihydrobenzo[b][1,4]dioxin-6-amine	4-NO_2	31.72±0.54
12	4-Aminophenyl(phenyl)methanone	H	27.52±0.07
13	4-Aminophenyl(phenyl)methanone	3-Br	35.12±0.42
14	4-Aminophenyl(phenyl)methanone	4-Br	36.32±0.52
15	4-Aminophenyl(phenyl)methanone	3-Cl	36.42±0.54
16	4-Aminophenyl(phenyl)methanone	4-Cl	36.27±0.28
17	4-Aminophenyl(phenyl)methanone	4-$N(CH_3)_2$	32.45±0.04
18	4-Aminophenyl(phenyl)methanone	4-F	27.75±0.35
19	4-Aminophenyl(phenyl)methanone	3-OCH_3	28.73±0.12
20	4-Aminophenyl(phenyl)methanone	4-OCH_3	28.62±0.08
21	4-Aminophenyl(phenyl)methanone	2-CH_3	27.32±0.64
22	4-Aminophenyl(phenyl)methanone	3-NO_2	36.25±0.25
23	4-Aminophenyl(phenyl)methanone	4-NO_2	26.22±0.71
24	2-Trifluoromethylanilines	2-Br	16.20±0.21
25	2-Trifluoromethylanilines	4-Cl	22.22±0.13
26	2-Trifluoromethylanilines	3-NO_2	21.22±0.11
27	2-Trifluoromethylanilines	4-NO_2	20.21±0.01

$$Potency(\%) = \frac{MIC(\mu g/mL) of\ reference}{MIC\ (\mu g/mL)\ of\ test\ compound} \times 100 \quad \ldots(9)$$

In both methods, the halogens, hydroxy, methoxy, and methyl-substituted imines were active against their microbial strains.

Antimalarial activities

The measured antimalarial actions of *E*-imine are tabulated in Table 6. Schiff bases **4**, **5**, **14-16**, and **22** exhibit respectable antimalarial actions referred to as *P. falciparum* stain. Here, the –I character of bromine, chlorine, and nitro auxiliaries enhances the antimalarial activity. Compounds **3**, **6**, **10**, **11**, **13**, and **17** produced modest antimalarial actions. The remaining *E*-imines show lesser antimalarial activity. This is due to the presence of dioxins, benzoyl groups, and halogens, hydroxy, methoxy, and nitro auxiliaries lowered the antimalarial actions.

Experimental Section

Materials and Methods

Utilized E-Merck, Hi-Media, and Sigma-Aldrich chemical company chemicals and solvents (E-Merck 99%, Hi-Media 98%, and Sigma-Aldrich 99% of purities) for this current investigation. Employed the Mettler FP51 melting point device with open glass capillaries for finding the melting points of prepared E-imines. Infrared spectroscopical data of entire *E*-imines were collected from Avatar-300 Thermo Nicolet Fourier Transform Infrared Spectrophotometer (32 scans, solid KBr form, 400-4000 cm^{-1}, 4 cm^{-1} resolution, and Thermo couple detectors) using KBr discs with a frequency range of 4000-400 cm^{-1}. Nuclear Magnetic Resonance spectroscopical data were collected from Bruker-AV 400 and 500 spectrometers operated at 400 M Hz. Applied 500 MHz for ^1H and 125 MHz for ^{13}C NMR spectra, employed d_6-$CDCl_3$ solvent & TMS as an internal standard. Micro-analysis of imines was collected from a Perkin-Elmer-240 type CHN analyzer. Mass spectral fragments of imines are collected in the Varian-Saturn 2200 GC-MS spectrometer, employing the FAB technique in chemical ionization mode.

General procedure for the synthesis of Schiff bases

About 2 mmol of 2,3-dihydro(b)[1,4]dioxin-6-amine or 4-benzoylaniline or 2-trifluoromethyl

aniline, substituted benzaldehydes and 0.3 g sulfated fly-ash:SnO_2 catalyst[25] were microwave irradiated at 550W for 3-6.5 m the period of 30 s [Samsung, GW73BD model, 230 V, 50 Hz, 100 N/750 W (ICE-705)] (Scheme 2). The feasibility of synthetic strategies was supervised by TLC. After completing, the reaction-product combination was extracted with 10 mL of dichloromethane. From simple filtration, the catalyst was departed. Solvent vaporization afforded the desired E-imines. Recrystallizing the raw imines using ethyl alcohol, giving glittering pale yellow solids, and they were kept in a desiccator.

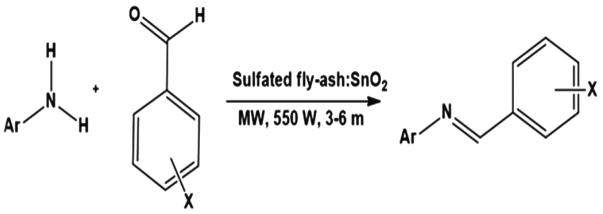

Entry	Ar	X
1-11	2,3-Dihydrobenzo[b][1,4]dioxin-6-yl	H, 3-Br, 4-Br, 3-Cl, 4-Cl, 4-F, 4-OH, 3-OCH_3, 2-CH_3, 3-NO_2, 4-NO_2
12-23	4-Benzoylphenyl	H, 3-Br, 4-Br, 3-Cl, 4-Cl, 4-$N(CH_3)_2$, 4-F, 4-OH, 3-OCH_3, 2-CH_3, 3-NO_2, 4-NO_2
24-27	2-Trifluoromethylphenyl	2-Br, 4-Cl, 3-NO_2, 4-NO_2

Scheme 2 — Sulfated fly-ash:SnO_2 catalyzed microwave irradiation assisted synthesis of *E*- imines

The prepared *E*-imines are analyzed with their physicochemical, micro-analysis, and spectroscopical information's and are presented in Table 7.

The spectral and analytical data of synthesized *E*-imines **1-11** are summarized below, and corresponding NMR spectra of compounds **1-11** and **24-27** are given in Figures S1- S30 (Supplementary Information). Moreover, mass spectra and mass fragments of compounds **1-11** and **24-27** are given in Figures S31- S60 (Supplementary Information).

(*E*)-N-Benzylidene-2,3-dihydrobenzo(*b*)[1,4]-dioxin-6-amine, 1: IR (KBr): 2917.11, 1582.07, 1462.31, 1067.54, 765.22 cm^{-1}; ^1H NMR (400 MHz, $CDCl_3$): δ 8.452(s, 1H, CH), 4.283(s, 4H, $(CH_2)_2$), 6.660-7.890(m, 9H, Ar-H). ^{13}C NMR (100 MHz, $CDCl_3$): δ 158.94 (CH), 64.20(CH_2), 64.72 (CH_2), 108.73-154.73 (Ar-C). Anal. Found (Calcd)(%): C

Table 7 — The physicochemical data, time-periods, and yield-quantity of made Schiff bases

Entry	Ar	X	MF	MW	Time (m)	Yield (%)	m.p. (°C)
1	2,3-Dihydrobenzo[b][1,4]dioxin-6-yl	H	$C_{15}H_{13}NO_2$	239	3.5	84	49-51
2		3-Br	$C_{15}H_{12}BrNO_2$	317	4.5	79	58-60
3		4-Br	$C_{15}H_{12}BrNO_2$	317	4.5	81	52-54
4		3-Cl	$C_{15}H_{12}ClNO_2$	273	4.5	76	44-46
5		4-Cl	$C_{15}H_{12}ClNO_2$	273	4	79	48-50
6		4-F	$C_{15}H_{12}FNO_2$	257	5	74	55-57
7		4-OH	$C_{15}H_{13}NO_3$	255	3	81	200-202
8		3-OCH_3	$C_{16}H_{15}NO_3$	269	3.5	86	62-64
9		2-CH_3	$C_{16}H_{15}NO_2$	253	4	80	46-48
10		3-NO_2	$C_{15}H_{12}N_2O_4$	284	5.5	75	118-120
11		4-NO_2	$C_{15}H_{12}N_2O_4$	284	5.5	79	122-124
12	4-Benzoylphenyl	H	$C_{20}H_{15}NO$	285	4.5	83	111-112(109-111)[21]
13		3-Br	$C_{20}H_{14}BrNO$	363	4	75	159-161(158-160)[21]
14		4-Br	$C_{20}H_{14}BrNO$	363	6	74	132-133(130-132)[21]
15		3-Cl	$C_{20}H_{14}ClNO$	319	3.5	78	108-109(106-108)[21]
16		4-Cl	$C_{20}H_{14}ClNO$	319	3	80	90-91(88-90)[21]
17		4-$N(CH_3)_2$	$C_{22}H_{20}N_2O$	328	3.5	83	139-141(138-140)[21]
18		4-F	$C_{20}H_{14}FNO$	302	5	76	100-101(98-100)[21]
19		3-OCH_3	$C_{21}H_{17}NO_2$	315	3	78	92-93(90-92)[21]
20		4-OCH_3	$C_{21}H_{17}NO_2$	315	3	82	98-99(96-98)[21]
21		2-CH_3	$C_{21}H_{17}NO$	299	4	79	106-107(104-106)[21]
22		3-NO_2	$C_{20}H_{14}N_2O_3$	330	5.5	72	110-111(108-110)[21]
23		4-NO_2	$C_{20}H_{14}N_2O_3$	330	5.5	77	142-143(140-142)[21]
24	2-Trifluoromethylphenyl	2-Br	$C_{14}H_9BrF_3N$	326	5	73	90-91
25		4-Cl	$C_{14}H_9ClF_3N$	283	4	76	121-122
26		3-NO_2	$C_{14}H_9BrF_3N_2O_2$	294	5.5	72	101-102
27		4-NO_2	$C_{14}H_9BrF_3N_2O_2$	294	4.5	72	115-116

,75.32 (75.30); H , 5.43 (5.48); N, 5.79 (5.85). MS: *m/z* 239[M^+], 162, 149, 135, 104, 91, 77, 30, 28, 14.

(*E*)-N-(3-Bromobenzylidene)-2,3-dihydrobenzo(b)[1,4]- dioxin-6-amine, 2: IR (KBr): 2958.18, 1581.44, 1427.15, 1063.41, 777.65 cm^{-1}; ^{1}H NMR (400 MHz, $CDCl_3$): δ 8.354(s, 1H, CH), 4.254(s, 4H, $(CH_2)_2$), 6.779-8.048(m, 8H, Ar-H). ^{13}C NMR (100 MHz, $CDCl_3$): δ 156.77 (CH), 64.19 (CH_2), 64.71 (CH_2), 104.20-144.96 (Ar-C). Anal. Found (Calcd)(%): C, 56.62 (56.60); H, 3.72 (3.76); N, 4.38 (4.36). MS: *m/z* 318[M^+], 320[M+2], 238, 182, 168, 162, 155, 149, 104, 135, 77, 30, 28, 14.

(*E*)-N-(4-Bromobenzylidene)-2,3-dihydrobenzo(b)[1,4]-dioxin-6-amine, 3: IR (KBr): 2979.21, 1586.71, 1424.70, 1044.35, 720.03 cm^{-1}; ^{1}H NMR (400 MHz, $CDCl_3$): δ 8.380(s, 1H, CH), 4.266(s, 4H, $(CH_2)_2$), 6.780-7.741(m, 8H, Ar-H). ^{13}C NMR (100 MHz, $CDCl_3$): δ 157.27 (CH), 64.20 (CH_2), 64.72 (CH_2), 104.20-145.21(Ar-C). Anal. Found (Calcd)(%): C, 56.59 (56.62); H, 3.74 (3.80); N, 4.40 (4.36). MS: *m/z* MS: *m/z* 318[M^+], 320[M+2], 238, 182, 177, 168, 162, 155, 149, 135, 103, 77, 30, 27, 14.

(*E*)−N-(3-Chlorobenzylidene)-2,3-dihydrobenzo(b)[1,4]-dioxin-6-amine, 4: IR (KBr): 2977.41, 1581.47, 1495.47, 1083.76, 778.86 cm^{-1}; ^{1}H NMR (400 MHz, $CDCl_3$): δ 8.362(s, 1H, CH), 4.245(s, 4H, $(CH_2)_2$), 6.778-7.884(m, 8H, Ar-H). ^{13}C NMR (100 MHz, $CDCl_3$): δ 156.86 (CH), 64.10 (CH_2), 64.70 (CH_2), 104.20-144.97(Ar-C). Anal. Found (Calcd)(%): C, 65.82 (65.85); H, 4.38 (4.42); N, 5.07 (5.12). MS: *m/z* 273[M^+], 275 [M+2], 238, 162,149, 138, 135, 132, 124, 111, 77, 35, 30, 27, 15.

(*E*)-N-(4-Chlorobenzylidene)-2,3-dihydrobenzo(b)[1,4]-dioxin-6-amine, 5: IR (KBr): 2976.23, 1581.91, 1425.61, 1065.54, 745.42 cm^{-1}; ^{1}H NMR (400 MHz, $CDCl_3$): δ 8.403(s, 1H, CH), 4.238(s, 4H, $(CH_2)_2$), 6.775.21-7.854.71(m, 8H, Ar-H). ^{13}C NMR (100 MHz, $CDCl_3$): δ 157.23 (CH), 64.20 (CH_2), 64.72 (CH_2), 104.25-145.25(Ar-C). Anal. Found (Calcd)(%): C, 65.79 (65.85); H, 4.40 (4.42); N, 5.13 (5.12). MS: *m/z* 273[M^+], 275 [M+2], 238, 162,149, 138, 135, 132, 124, 111, 77, 35, 30, 28, 14.

(*E*)-N-(4-Fluorobenzylidene)-2,3-dihydrobenzo(b)[1,4]-dioxin-6-amine, 6: IR (KBr): 2978.60, 1588.29, 1495.99, 1092.97, 798.18 cm^{-1}; ^{1}H NMR (400 MHz, $CDCl_3$): δ 8.397(s, 1H, CH), 4.163 (s, 4H, $(CH_2)_2$), 6.184.-7.883(m, 8H, Ar-H). ^{13}C NMR (100 MHz, $CDCl_3$): δ 157.31 (CH), 64.19 (CH_2), 64.70 (CH_2), 104.24-145.44(Ar-C). Anal. Found (Calcd)(%): C, 69.98 (70.03); H, 4.68 (4.70); N, 5.38 (5.44). MS: *m/z* 257[M^+], 259 [M+2], 238, 162, 149, 135,122, 116, 108, 95, 77, 30, 28, 27, 19, 14.

(*E*)-N-(4-Hydroxybenzylidene)-2,3-dihydrobenzo(b)[1,4]-dioxin-6-amine, 7: IR (KBr): 2917.93, 1584.90, 1432.91, 1086.09, 799.83 cm^{-1}; ^{1}H NMR (400 MHz, $CDCl_3$): δ 8.362(s, 1H, CH), 4.236 (s, 4H, $(CH_2)_2$), 6.197.-7.790(m, 8H, Ar-H). ^{13}C NMR (100 MHz, $CDCl_3$): δ 157.99 (CH), 63.72 (CH_2), 63.80 (CH_2), 104.90-145.04(Ar-C). Anal. Found (Calcd)(%): C, 69.52 (70.58); H, 5.09 (5.13); N, 5.44 (5.49). MS: *m/z* 255[M^+], 238, 162, 149, 135, 120, 114, 106, 93, 77, 30, 28, 27, 17.

(*E*)-N-(3-Methoxybenzylidene)-2,3-dihydrobenzo(b)[1,4]-dioxin-6-amine, 8: IR (KBr): 2987.03, 1591.19, 1465.21, 1065.28, 795.01 cm^{-1}; ^{1}H NMR (400 MHz, $CDCl_3$): δ 8.359(s, 1H, CH), 4.252 (s, 4H, $(CH_2)_2$), 3.846 (s, 3H, OCH_3), 6.754-7.818(m, 8H, Ar-H). ^{13}C NMR (100 MHz, $CDCl_3$): δ 158.31 (CH), 64.19 (CH_2), 64.71 (CH_2), 55.41(OCH_3), 104.17-146.07(Ar-C). Anal. Found (Calcd) (%): C, 69.52 (69.48); H, 5.09 (5.06); N, 5.44 (5.39). MS: *m/z* 269[M^+], 254, 238, 162, 149, 135, 134, 120,119, 107, 91, 77, 31, 27, 15, 14.

(*E*)-N-(2-Methylbenzylidene)-2,3-dihydrobenzo(b)[1,4]-dioxin-6-amine, 9: IR (KBr): 2975.14, 1582.09, 1467.48, 1083.56, 754.74 cm^{-1}; ^{1}H NMR (400 MHz, $CDCl_3$): δ 8.539(s, 1H, CH), 4.192 (s, 4H, $(CH_2)_2$), 2.814 (s, 3H, CH_3), 6.721-8.046(m, 8H, Ar-H). ^{13}C NMR (100 MHz, $CDCl_3$): δ 157.65 (CH), 64.20 (CH_2), 64.72 (CH_2), 29.75(CH_3), 104.25-146.39(Ar-C). Anal. Found (Calcd) (%): C, 75.88 (75.92); H, 5.93 (5.97); N, 5.48 (5.53). MS: *m/z* 253[M^+], 238, 162, 149, 135, 118, 112, 104, 91, 77, 30, 27, 15, 14.

(*E*)-N-(3-Nitrobenzylidene)-2,3-dihydrobenzo(b)[1,4]-dioxin-6-amine, 10: IR (KBr): 2988.17, 1584.54, 1484.25, 1085.35, 759.21 cm^{-1}; ^{1}H NMR (400 MHz, $CDCl_3$): δ 8.521(s, 1H, CH), 4.291 (s, 4H, $(CH_2)_2$), 6.836-8.303(m, 8H, Ar-H).

^{13}C NMR (100 MHz, $CDCl_3$): δ 155.31 (CH), 64.13 (CH_2), 64.73 (CH_2), 104.87-146.32(Ar-C). Anal. Found (Calcd) (%): C, 63.40 (63.38); H, 5.19 (4.25); N, 5.48 (5.42). MS: *m/z* 284[M^+], 238, 162, 149, 143, 135,122, 103, 89, 77, 46, 30, 28, 27, 14.

(*E*)-N-(4-Nitrobenzylidene)-2,3-dihydrobenzo(b)[1,4]-dioxin-6-amine, 11: IR (KBr): 2992.01, 1579.22, 1492.57, 1090.87, 792.87 cm^{-1}; ^{1}H NMR (400 MHz, $CDCl_3$): δ 8.521(s, 1H, CH), 4.291(s, 4H, $(CH_2)_2$), 6.836-7.744(m, 8H, Ar-H). ^{13}C NMR (100 MHz, $CDCl_3$): δ 155.29 (CH), 64.18 (CH_2), 64.70 (CH_2), 104.17-148.67(Ar-C). Anal. Found (Calcd) (%): C, 63.35 (63.38); H, 5.22 (4.25); N, 5.39 (5.42). MS: *m/z* 284[M^+], 238, 162, 149, 143,135, 122, 77, 30, 28, 27, 19, 15.

(*E*)-N-(2-Bromobenzylidene)-2-(trifluoromethyl)aniline, 24: IR (KBr): 3071.30, 1580.44, 1371.77, 1110.70, 752.90 cm^{-1}; ^{1}H NMR (400 MHz, $CDCl_3$): δ 8.786(s, 1H, CH), 7.098-7.711(m, 9H, Ar-H). ^{13}C NMR (100 MHz, $CDCl_3$): δ 160.54 (CH), 150.32 (CN), 122.56 (CF_3), 119.48-134.35(Ar-C). Anal. Found (Calcd) (%): C, 51.32 (51.25); H, 2.82 (2.76); N, 4.32 (4.27). MS: *m/z* 328[M^+], 330[M^{2+}], 332[M^{+4}], 334[M^{+6}], 336[M^{+8}], 258, 248, 182, 171, 168, 159, 156, 145, 79, 69, 27, 19, 15.

(*E*)-N-(4-Chlorobenzylidene)-2-(trifluoromethyl)aniline, 25: IR (KBr): 3071.30, 1577.80, 1401.21, 1118.20, 735.21 cm^{-1}; ^{1}H NMR (400 MHz, $CDCl_3$): δ 8.339(s, 1H, CH), 7.036-7.874(m, 9H, Ar-H). ^{13}C NMR (100 MHz, $CDCl_3$): δ 160.00 (CH), 150.39 (CN), 122.34 (CF_3), 119.23-138.01(Ar-C). Anal. Found (Calcd) (%): C, 59.34 (59.28); H, 3.23 (3.20); N, 4.92 (4.94). MS: *m/z* 283[M^+], 285[M^{2+}], 287[M^{4+}], 289[M^{6+}], 291[M^{8+}], 247, 213, 171, 158, 145, 137, 124, 111, 76, 69, 35, 27, 19, 15.

(*E*)-N-(3-Nitrobenzylidene)-2-(trifluoromethyl)aniline, 26: IR (KBr): 3078.33, 1580.47, 1312.00, 1125.70, 758.20 cm^{-1}; ^{1}H NMR (400 MHz, $CDCl_3$): δ 8.696(s, 1H, CH), 7.068-8.373(m, 9H, Ar-H). ^{13}C NMR (100 MHz, $CDCl_3$): δ 158.75 (CH), 149.61 (CN), 124.09 (CF_3), 119.03-148.70(Ar-C). Anal. Found (Calcd) (%): C, 61.43 (61.44); H, 3.43 (3.44); N, 4.75 (4.78). MS: *m/z* 293[M^+], 295[M^{+2}], 297[M^{+4}], 299[M^{+6}], 247, 224, 171, 158, 148, 135, 122, 102, 76, 69, 46, 27, 19, 15.

(*E*)-N-(4-Nitrobenzylidene)-2-(trifluoromethyl)aniline, 27: IR (KBr): 3116.10, 1595.30, 1312.20, 1110.70, 794.12 cm^{-1}; ^{1}H NMR (400 MHz, $CDCl_3$): δ 8.479(s, 1H, CH), 7.080-8.338(m, 9H, Ar-H). ^{13}C NMR (100 MHz, $CDCl_3$): δ 158.84 (CH), 149.65 (CN), 124.06 (CF_3), 118.85-149.55(Ar-C). Anal. Found (Calcd) (%): C, 61.39 (61.44); H, 3.41 (3.44); N, 4.79 (4.78). MS: *m/z* 293[M^+], 295[M^{2+}], 297[M^{4+}], 299[M^{6+}], 247, 224, 171, 158, 148, 145, 135, 122, 69, 76, 46, 30, 27, 19, 15.

Molecular docking computation

Employing ChemDraw-12 software for drawing the structure-assembly of Schiff bases. Babel software was used for structure optimization and conversion to PDB form, then archived for the molecular docking experiment. From the Protein Data Bank (PDB) (www.rcsb.org) HER2 protein inhibitor (PDB: 7PCD)[26-28], the 3D final assembly was taken. Receptor preparation stages are, first level is the deletion of hetero-atoms (H_2O and charged particles), second level is the accumulation of protons, and then the assessment of charges. Dynamic and active regions were found from the lattice network cases with precise dimensions of assured ligands. Employed Auto Dock Vina software and Discovery Studio visualization for docking experiments, finding 2D and 3D docking assemblies. The binding energies of all *E*-imines with the above-said proteins are presented in Table 8.

Determination of Antimicrobial Potencies

From Bauer-Kirby[29] disc diffusion procedure, assess the antimicrobial potencies of Schiff bases **1-11** and **24-27**. In this process, three Gram-positive and two Gram-negative microorganisms, namely, *B. subtilis*, *S. aureus*, *S. pyogenes*, *E. coli*, and *P. aeruginosa* were utilized for measuring the antibacterial actions of these imines. About three antifungal microbes namely, *A. niger*, *F. oxysporum*, and *P. chrysogenum* used for measuring the antifungal activity of the imines. The standard drugs Ciprofloxacin and Clotrimazole were employed in these experiments.

Applied a double successive dilution process for finding the minimum inhibitory concentration (MIC). The antibacterial activities of *E*-imines using the MIC evaluation test were completed in the sowed broth (10^{-6} to 10^{-7} (CFU/ mL). Incorporated the dissimilar strengths of imines such as 180, 90, 45, 22.5, 11.25, 5.62, 2.18, 1.40, 0.70, and 0.35 μg/mL for finding the

Table 8 — The binding energies (ΔG, kcal/mol) of *E*-imines with proteins

Entry	Ar	X	Binding energy
1	2,3-Dihydrobenzo[b][1,4]dioxin-6-yl	H	–5.34
2	2,3-Dihydrobenzo[b][1,4]dioxin-6-yl	3-Br	–5.88
3	2,3-Dihydrobenzo[b][1,4]dioxin-6-yl	4-Br	–5.98
4	2,3-Dihydrobenzo[b][1,4]dioxin-6-yl	3-Cl	–6.14
5	2,3-Dihydrobenzo[b][1,4]dioxin-6-yl	4-Cl	–5.19
6	2,3-Dihydrobenzo[b][1,4]dioxin-6-yl	4-F	–5.72
7	2,3-Dihydrobenzo[b][1,4]dioxin-6-yl	4-OH	–6.14
8	2,3-Dihydrobenzo[b][1,4]dioxin-6-yl	3-OCH_3	–5.55
9	2,3-Dihydrobenzo[b][1,4]dioxin-6-yl	2-CH_3	–5.57
10	2,3-Dihydrobenzo[b][1,4]dioxin-6-yl	3-NO_2	–6.25
11	2,3-Dihydrobenzo[b][1,4]dioxin-6-yl	4-NO_2	–6.27
12	4-Benzoyl phenyl	H	–7.51
13	4-Benzoyl phenyl	3-Br	–8.38
14	4-Benzoyl phenyl	4-Br	–8.07
15	4-Benzoyl phenyl	3-Cl	–8.02
16	4-Benzoyl phenyl	4-Cl	–8.27
17	4-Benzoyl phenyl	4-$N(CH_3)_2$	–8.21
18	4-Benzoyl phenyl	4-F	–7.75
19	4-Benzoyl phenyl	3-OCH_3	–7.67
20	4-Benzoyl phenyl	4-OCH_3	–8.04
21	4-Benzoyl phenyl	2-CH_3	–7.82
22	4-Benzoyl phenyl	3-NO_2	–8.17
23	4-Benzoyl phenyl	4-NO_2	–6.22
24	2-Trifluoromethylphenyl	2-Br	–4.98
25	2-Trifluoromethylphenyl	4-Cl	–4.50
26	2-Trifluoromethylphenyl	3-NO_2	–5.66
27	2-Trifluoromethylphenyl	4-NO_2	–5.57

minimum inhibitory concentration (MIC). As well as the reference ciprofloxacin drug liquid with sterilized water (μg/mL) was made at the above concentration range with the regulator reagent DMSO. The whole MIC determination method comprised an order of 10 assay-processing glass tubes for the prepared *E*-imines, in contrast to microorganisms. In the first assay-processing glass-tube, 1.5 mL of the sowed broth and 0.45 mL of the *E*-imine were then made to 180 μg/mL. Similarly, the remaining nine assay-processing glass tubes with a desired quantity of broths and compounds. From this to prepared the third tube and onwards up to the tenth tube. Under aseptic conditions, this work was done in duplicates. The prepared assay tubes were incubated under the temperature of 37 ± 1°C for 24 h. Over the incubation process, the strength of the serially diluted tubes was marked with an agar plate to avoid turbidity. MIC was calculated as the lowest concentration of *E*-imine that causes whole blocking of the development of corresponding strains. Besides the regulator-solvent assay, the process glass tube was monitored during the inhibitory action. Sterilized distilled water and the solvent DMSO do not involve inhibition. The above two-fold serial dilution technique and Bauer-Kirby disc diffusion process were incorporated for assessing antimicrobial activity of *E*-imines **1-11** and **24-27**.

To evaluate the antifungal activities of synthesized *E*-imines, the development of fungi and the examination were conducted in the medium of sabouraud dextrose agar (SDA) and sabouraud dextrose broth (SDB) medium[30,31]. A similar procedure was done in antibacterial studies, followed by performing subculture and viable counts. These should be maintained at the temperature range of 28 ± 1°C for about 72 h for assessing MIC, as well as in mm of the zone of inhibition of Petri dishes in the disc diffusion method. The identical concentration of the *E*-imines (**1-11** and **24-27**), DMSO is a regulating reagent, and Clotrimazole, as a reference, made formerly was followed to assess the MIC.

Antimalarial activity of imines

The procedure reported in the literature was applied for assessment of antimalarial potencies of all imines. The Thailand strain *P. falciparum* microorganism K1 employed for cultures development of cell[20,32-34]. The development of cultures in entire medium containing RPMI1640

accompanied 11 mM of glucose, 27.5 mM of H_2CO_3, 100 µL/mL of each streptomycin, penicillin and 8% of human serum albumin (heat-inactivated). Growth change of parasites were done in the temperature of 37 °C along with human A+ red blood cells (RBCs) on 2% hematocrit, lower than 3% CO_2, 6% O_2, & 91% N_2 combinations. Giemsa-stained smears utilized for the evaluation of *in-vitro* assay of cultures with 3-6% parasitemia by numeration of parasites. The development growth experiment were conducted as follows. The increasing strength of the *E*-imines was prepared with DMSO, and the conducted inhibitory action against the intraerythrocytic growth *of P. falciparum*. In a candle jar, the parasites were grown at a temperature of 37 °C for 24h along with the well containing 0.5µCi ^{3}H-hypoxanthine. After 24 h incubation, the freeze-thawed dishes were collected. The 1450Micro-beta counter was employed to counter the wetted scintillation culture. The percentage of growth embarrassment was calculated by suitable and responding radio waves of a parasite. Cent percent assimilation of ^{3}H-hypoxanthine was found by growth regulation in the absence of *E*-imines. The IC_{50} values were calculated by the mean strength found by the non-identical test groups.

Conclusions

There are three series of greater than 70% yields of *E*-imines namely (*E*)-N-(substituted benzylidene)-2,3-dihydrobenzo(*b*)[1,4]-dioxin-6-amines, (*E*)-[4-(substituted benzylideneamino) phenyl] (phenyl) methanones and (*E*)-N-(substituted benzylidene)-2-(trifluoromethyl)anilines were synthesized by sulfated fly-ash:SnO_2 catalyst assisted condensation of 2,3-dihydrobenzo(*b*)[1,4]-dioxin-6-amine, 4-benzoyl aniline with aldehydes under microwave irradiation conditions. These are examined by their physicochemical numerations and spectroscopical information's. X-Ray Diffraction geometry of (*E*)-N-(4-nitrobenzylidene)-2-(trifluoromethyl)aniline (**27**) was established. From the single regression analysis of characteristic spectral frequencies, the infrared CN stretches (ν, cm^{-1}) and proton chemical shifts (δ, ppm) of -CH=N- gave an acceptable correlation coefficient with resonance components. The carbon-13 chemical shifts (δ, ppm) of -CH=N- gave satisfactory correlations with all sigma F and R numerations. Dolby line statistical computations of all frequencies provide acceptable correlation coefficients against Swain-Lupton's parameters. Imines **4**, **7**, **10**, **11**, **13**, **16**, **17**, and **22** show high protein-ligand interaction binding energy in docking investigations. The (*E*)-N-(4-chlorobenzylidene)-2,3-dihydrobenzo(*b*)[1,4]-dioxin-6-amines **5-7** and **10** exhibit good antibacterial actions in contrast with *S. aureus*, *S. pyogenes*, *and E.coli* microorganisms. From the serial dilution method, all compounds are active against their antibacterial strains. The imines **2-9**, **24**, and **26** were active with MICs of 9.5-16.5 against A. *niger* microbes. The +I, –I, +R, electronegativity, and hyper-conjugation effects of bromine, chlorine, methoxy, nitro, fluorine, and methyl groups cause antimicrobial activity. Imines **4**, **5**, **14-16**, and **22** exhibit respectful anti-malarial actions in contrast with the *P. falciparum* organism.

Supplementary Information

Supplementary information is available in the website https://nopr.niscpr.res.in/handle/123456789/58776.

Acknowledgments

Authors thank (i). DST-NMR Facility, Department of Chemistry Annamalai University, Annamalainagar-608 002 for recording NMR spectra of all imines and (ii) Thank RUSA-2, Field 1, Anti-Malarial Drug Synthesis, No. F3/RUSA/673/2022, dated 4-6-2022, Annamalai University, Annamalainagar-608002, for financial support.

References

1 Kamalakkannan D, Senbagam R, Vanangamudi G & Thirunarayanan G, *J Mol Struct*, 1264 (2022) 133218.
2 Meyer C D, Steven Joiner C & Fraser Stoddart J, *Chem Soc Rev*, 36 (2007) 1705.
3 Collados J F, Toledano E, Guijarro D & Yus M, *J Org Chem*, 77 (2012) 5744
4 Yu C, Bu J, Wang W, Shen H, Cao H & Zhang H, *Ind Eng Chem Res*, 61 (2022) 5442.
5 Abid M, Savolainen M, Landge S Hu J, Surya Prakash G K, George A, Olah C & Török B, *J Flu Chem*, 128 (2007) 587.
6 Zuo Z, Liu J, Nan J, Fan L, Sun W, Wang Y & Luan X, *Angew Chem Int Ed Eng*, 54 (2015) 15385
7 Rizzuti A, Dipalo M C, Allegretta I, Terzano R, Cioffi N, Mastrorilli P, Matilda M, Giuseppe R. Angelo N & Dell Anna M M, *Catalysts*, 10 (2020) 1325.
8 Pal A, Das M K & Thakur A, *J Org Chem*, 88 (2023) 8955.
9 Wu S, Sun W, Chen J, Zhao J, Cao Q, Fang W & Zhao Q, *J Catal*, 377 (2019) 110.
10 Hashimoto T, Kimura H, Kawamata Y & Maruoka K, *Nature Chem*, 3 (2011) 642.
11 Chu G & Li C, *Org Biomol Chem*, 8 (2010) 4716.
12 Rajarajan M, Pachamuthu M P, Thirunarayanan G, Vanangamudi & Hamdy M S, *S N Appl Sci*, 1 (2019) 940.
13 Thirunarayanan G, Mayavel P, Thirumurthy K, Vanangamudi G, Sekar K G & Lakshmanan K, *J Chil Chem Soc*, 58 (2013) 2231.

14 Mayavel P, Thirumurthy K, Dineshkumar S & Thirunarayanan G, *Indian J Chem*, 54B (2015) 779.
15 Sakthinathan S P, Suresh R, Kamalakkannan D, Mala V, Sathiyamoorthi K, Vanangamudi G & Thirunarayanan G, *J Chil Chem Soc*, 63 (2018) 3918
16 Messasma Z, Aggoun D, Houchi S, Ourari A, Ouennoughi Y, Keffous F & Mahdadi R, *J Mol Struc*, 1228 (2021) 129463.
17 Celik S, Ozkok F, Ozel A E, Cakir E & Akyuz S, *J Mol Struc*, 1236 (2021) 130288.
18 Dinesh kumar N, Thirunarayanan G, Elancheran R, Suppuraj P, Guganathan L, Sivasakthikumar R, Ramkumar S & Swaminathan M, *J Mol Struc*, 1322 (2025) 140603.
19 Dinesh kumar N, Swaminathan M, Selvakumar K, Durai M, Muthuvel I, Ebaid H, Krishnakumar B, Ahn Y H & Thirunarayanan G, *J Mol Struc*, 1325 (2025) 140918.
20 Mariene H D, Stephen J B & Matheus P F, *Comb Chem High Throughput Screen*, 18 (2015) 208.
21 Mayavel P, Thirumurthy K, Dineshkumar S & Thirunarayanan G, *Int Lett Chem Phys Astro*, 39 (2014) 145.
22 Thirunarayanan G & Sekar K G, *J Saudi Chem Soc*, 20 (2016) 661.
23 Thirunarayanan G & Ananthakrishna Nadar P, *J Indian Chem Soc*, 83 (2006) 1107.
24 Swain C G & Lupton E C J, *J Am Chem Soc*, 90 (1968) 4328.
25 Thirumurthy K & Thirunarayanan G, *RSC Adv*, 5 (2015) 33595.
26 Elkhalifa A E O, Al-Shammari E, Kuddus M, Adnan M, Sachidanandan M, Awadelkareem A M, Qattan M Y, Idreesh Khan M & Abduljabbar S I, *Life*, 13 (2023) 1739.
27 Renadi S, Kusuma Pratita A T, Mardianingrum R & Ruswanto R, *J Kimia Valensi*, 9 (2023) 89.
28 Septian A D, Wardani G A, Mardianingrum R & Ruswanto R, *J Kimia Valensi*, 9 (2023) 163.
29 Bauer A W, Kirby W M M, Sherris J C & Truck M, *Am J Clin Pathol*, 45 (1966) 493.
30 Muthuvel I, Divya J, Gayathri P, Balasundari S, Sudha P, Palanivel C, Krishnakumar B, Manikandan V, Alanazi A K, & Thirunarayanan G, *Indian J Chem*, 64 (2025) 942.
31 Gayathri P, Koteswara R A, Divya J, Balasundari S, Sudha P, Mayavel P, Muthuvel I, Usha V, Sathiyendiran V, Krishnakumar B, Ranganathan K, Kumar N D, Rajasri S & Thirunarayanan G, *Indian J Chem*, 64 (2025) 1097.
32 Agniv P & Dipak C, *Curr Trend Pharm Res*, 8 (2021) 2582.
33 Aliasghar J, Edris E, Véronique S, Christine L & Jean M B, *Eur J Med Chem*, 87(2014) 364.
34 Neda F, Shahin A, Lotfollah S, Somayeh E & Mahboubeh R, *Am J Biomed Sci Res*, 16 (2022) 321.